Geophysical Journal International

Geophys. J. Int. (2019) **218,** 1456–1468
Advance Access publication 2019 May 08
GJI Seismology

doi: 10.1093/gji/ggz208

Study of the regional pattern of intrinsic and scattering seismic attenuation in Eastern Sicily (Italy) from local earthquakes

E. Del Pezzo [1,2] E. Giampiccolo [3] T. Tuvé,[3] G. Di Grazia,[3] S. Gresta[4] and J.M. Ibàñez[2,3]

[1] *INGV Osservatorio vesuviano. Via Diocleziano,* 328. 80124 *Napoli, Italy*
[2] *Andalusian Institute of Geophysics. University of Granada,* 18071. *Granada, Spain*
[3] *INGV Osservatorio Etneo. Piazza Roma* 2, *Catania, Italy. E-mail: elisabetta.giampiccolo@ingv.it*
[4] *Dipartimento di Scienze Biologiche, Geologiche e Ambientali, Università di Catania, Corso Italia,* 57 *Catania, Italy*

Accepted 2019 May 6. Received 2019 March 19; in original form 2018 November 20

SUMMARY

The mechanism of seismic attenuation for shear waves was studied through the separate measure of the intrinsic dissipation and scattering coefficients. A modified version of the Multiple Lapse Time Window Analysis (MLTWA) was applied to about 5000 local earthquakes with magnitude $1.5 \leq \mathrm{Ml} \leq 4.8$ occurred in the period 2006–2017 in both the tectonic (Peloritani Mountains and Hyblean Plateau) and volcanic (Aeolian Islands and Mt Etna) areas of eastern Sicily. Observed data, processed via direct Fourier Transform instead of the filtering and averaging procedures utilized in the ordinary MLTWA technique, were fit to the correspondent Paasschens solution of the Energy Transport model in 3D. Model parameters B_0, the seismic albedo, and Le, the extinction length, in turn associated with the intrinsic (Q_i) and scattering (Q_s) quality factors for S waves, are thus obtained from the fit in the frequency bands centred at 1.5, 3, 6 and 12 Hz. Finally, the corrections to these estimates in case of an opaque layer (the crust) overlying a uniform and transparent mantle, were applied in order to obtain more realistic estimates of the seismic attenuation in the areas investigated. Obtained results are first interpreted in terms of the characteristics of each domain and then compared by the same point of view with a huge set of measurements of the same parameters carried out in other tectonic and volcanic domains through the world. Results show how the rock heterogeneity characterizes the tectonic domain and determines the value of total attenuation coefficient, which, on the other hand, is a crucial parameter in the estimation of the seismic hazard.

Key words: Fourier analysis; Earthquake hazards; Seismic attenuation; Wave scattering and diffraction.

INTRODUCTION

Seismic attenuation severely influences ground motion and hence earthquakes damage. As a consequence, its evaluation in seismically active areas is mandatory for the correct estimation of the earthquake hazard. On the other hand, the quantification of the seismic attenuation parameters is required for correcting seismic source spectra, the observational basis of the seismic source studies.

The attenuation of seismic waves can be described by the total quality factor, Q_t which implicitly takes into account all the energy lost by the primary waves along the Fermat's path during the wave propagation. $Q_t = 2\pi f/(v\eta)$, where f is the frequency and v is the wave speed, is inversely proportional to the attenuation coefficient η and takes into account the overall effects of both intrinsic absorption and scattering attenuation: $Q_t^{-1} = Q_i^{-1} + Q_s^{-1}$. Q_i^{-1} accounts for conversion of the seismic wave energy into heat due to the presence in the Earth medium of abnormal structural defects (i.e. microcracks and cavities, either fluid filled or not) with dimension very small compared to the seismic wavelength. Q_s^{-1} describes the energy lost by the primary wave and converted to secondary waves (scattering) due to the presence of medium heterogeneities (Sato *et al.* 2012).

Quantifying the relative contribution of intrinsic and scattering attenuation to the total quality factor, Q_t^{-1}, is important to understand the phenomena of wave propagation and helps in the seismogram synthesis, as the scattering phenomena actually redistribute the energy which apparently is lost in the primary wave front, into the seismogram coda: the overall effect is to affect the duration of ground shacking, a crucial parameter in seismic hazard studies. This is the reason why the separate estimate of Q_i and Q_s has been the subject of considerable interest among seismologists in the last decades (see

e.g. Carcolé & Sato 2010). Several methods have been proposed in the past to separately estimate Q_i^{-1} and Q_s^{-1} (i.e. Wu 1985; Frankel & Wennerberg 1987; Wennerberg 1993) even though the most popular method is the Multiple Lapse Time Window Analysis (MLTWA; Hoshiba *et al.* 1991; Fehler *et al.* 1992). This technique is based on the normalization of the seismogram Energy envelopes for the coda amplitude at a given fixed lapse time [the so called 'coda normalization' (CN), that allows to normalize for the source intensity]. The theoretical (normalized) energy is well described by the Paasschens' solution (Paasschens 1997) of the Energy Transport (Boltzmann) equation (hereafter ET). More recently, Eulenfeld & Wegler (2016) used an approach different from MLTWA, obtaining stable and robust estimates of separated attenuation parameters, jointly with source and site properties. MLTWA maintains however its validity and can be still considered as a valid tool. MLTWA has been widely applied in several tectonically and volcanically active regions worldwide (e.g. Mayeda *et al.* 1992; Giampiccolo *et al.* 2006; Tuvé *et al.* 2006; Ugalde *et al.* 2007; Badi *et al.* 2009; Del Pezzo *et al.* 2011; Padhy & Subhadra 2013; Del Pezzo *et al.* 2015; Singh *et al.* 2017). It is based on the comparison among the pattern of the time integral of the signal energy, calculated in different successive time windows along the coda, as a function of source–receiver distance of local earthquakes, and the corresponding theoretical values calculated on the basis of the scalar approximation of the radiative transfer theory applied to scalar waves (Sato & Fehler 1998).

In this paper, we applied a slightly modified version of MLTWA to about 5000 local earthquakes which occurred in the period 2006–2017 in both the tectonic (Peloritani Mountains and Hyblean Plateau) and volcanic (Aeolian Islands and Mt Etna) areas of eastern Sicily, which is a seismically very active and tectonically very complex area, characterized by a high seismic risk.

While for Mt Etna, Peloritani Mountains and Hyblean Plateau previous estimates of separated intrinsic and scattering attenuation parameters have been already published (Giampiccolo *et al.* 2004, 2006; Tuvé *et al.* 2006; Del Pezzo *et al.* 2015), there are still no studies on attenuation of seismic waves in the Aeolian Islands region. The studies so far carried out in Eastern Sicily suffer from a lack of homogeneity among approaches used, datasets and instrumental characteristics. The present availability of a high quality local earthquakes data set, recorded in the whole of Eastern Sicily by a dense and well-designed seismic network installed starting from 2006, prompted us to re-evaluate the crustal attenuation characteristics of the whole region by carrying out a detailed seismic attenuation study based on homogeneous data, in order to better compare the zones investigated. It is worth mentioning that a critical point in ordinary MLTWA applications is the half-space model assumption (constant velocity and attenuation parameters versus depth), as the Earth structure is in general far from being homogeneous in depth. A better assumption is thus an earth model characterized by an inhomogeneous crust overlying an almost homogeneous mantle (e.g. Hoshiba *et al.* 2001). In the present paper we estimate the amount of bias due to the simplistic half-space assumption following the scheme described in Del Pezzo & Bianco (2010a).

The present paper: (i) shows a reappraisal of the seismic attenuation parameters in Eastern Sicily; (ii) adds new and homogeneous information for the area of Aeolian Islands; (iii) estimates the bias associated with the attenuation parameters obtained under the assumption of half-space instead of a more realistic earth structure with most of scattering phenomena occurring in the crust; (iv) compares the attenuation parameters with those estimated worldwide using the same MLTWA technique and (v) gives more stable and reliable seismic attenuation estimates for the whole Eastern Sicily to be utilized for seismic hazard applications.

TECTONIC SETTING AND SEISMICITY

Eastern Sicily (Fig. 1) represents a geologically complex area in which several geodynamic processes associated with the convergence between Eurasian and Nubian plates coexist: lithospheric subduction, continen–continent collision, strike-slip margins and continental rifting (Cavazza & Wezel 2003; McClusky *et al.* 2003; Mauffret 2007; Palano *et al.* 2012; De Guidi *et al.* 2014). The whole area can be subdivided into four domains: (a) Southern Tyrrhenian domain (Aeolian Islands; Fig. 1a), characterized by an island arc associated with a subduction zone; (b) Peloritani Mountain Chain (Fig. 1b), part of the Calabro-Peloritan Arc extending from the northern edge of Calabria to northeastern Sicily, representing a major tectonic structure in southern Italy; (c) Mt Etna volcano (Fig. 1c), the most important volcanic structure of Mediterranean area, extending from Peloritani Mountains to the Hyblean Mountains in the south and (d) Hyblean Plateau (Fig. 1d), part of the orogenic foreland deformed by extensional and strike-slip faults.

From the seismic point of view, the Southern Tyrrhenian domain (Aeolian Islands; Fig. 1a) is characterized, in the eastern and central sectors, by a crustal seismicity, with sources in the upper 20 km, associated with two main fault systems, the WNW–ESE striking Sisifo-Alicudi system (SA) and the NNW–SSE striking ATLF system (Neri *et al.* 1996; De Luca *et al.* 1997). Intermediate and deep earthquakes affect the western area and are associated with the subduction of the Calabrian arc towards the west.

The Peloritani Mountains region (Fig. 1b) is one of the most seismically active areas in Italy, and it is characterized by the occurrence of crustal events (depth < 35 km) with magnitudes up to 7.2 and intensities of up to XI–XII MCS (Azzaro *et al.* 2007).

Mt Etna volcano-tectonic seismicity (VT hereafter; Fig. 1c) mainly occurs in the shallower crust (depth < 10 km) with a high rate of earthquakes of low and moderate magnitude, which rarely exceed 4.0 (Patanè & Giampiccolo 2004). Intermediate events ($5 \leq H \leq 15$ km) predominantly occur on the western flank whereas, the deep seismicity ($15 \leq H \leq 35$ km) is mostly confined to the northwestern sector of the volcano (Fig. 1c; Sicali *et al.* 2014 and references therein).

The seismicity in the Hyblean Plateau area (Fig. 1d) is sparse in space and time. The main seismic activity of the region is related to the faults segments conjugated to the NNW–SSE oriented Malta Escarpment Fault System (MEFS), whereas weaker shocks are due to the secondary inland faults (Bianca *et al.* 1999; Azzaro & Barbano 2000; Brancato *et al.* 2009). In the central sector of the Hyblean Plateau seismicity is almost absent. A detailed description of the tectonic and seismic characteristics of each domain, together with all the necessary references, is presented as Supporting Information.

METHOD

The MLTWA is essentially a numerical technique to fit the Seismogram Energy Time Envelopes calculated as a function of source–receiver distance to the correspondent theoretical ET, in order to characterize the propagation medium in terms of intrinsic dissipation and scattering coefficients, or, equivalently, the seismic albedo,

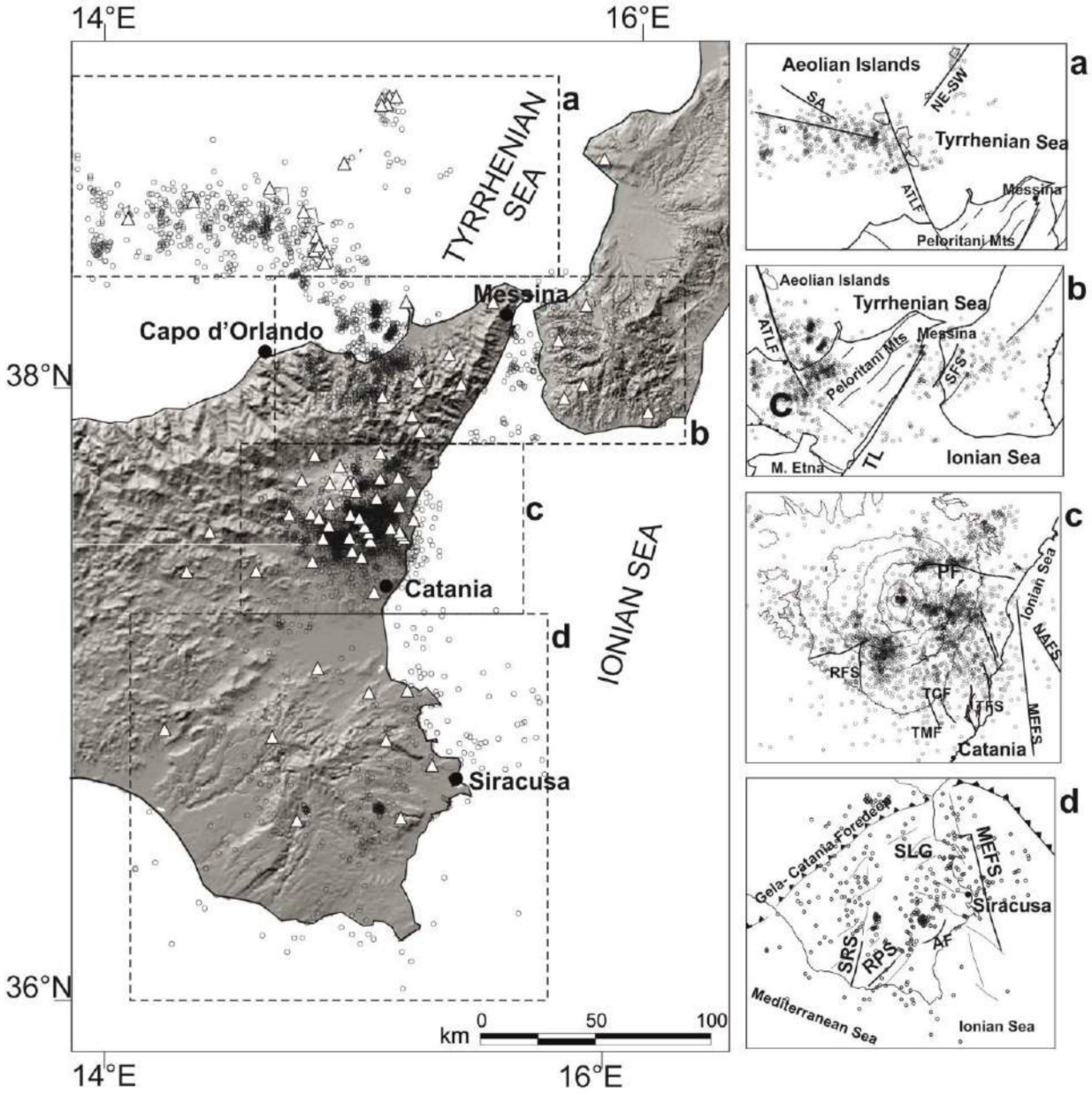

Figure 1. Map of Eastern Sicily and distribution of the earthquakes selected for this study (empty circles). White triangles represent the locations of seismic stations. Dashed boxes enclose the study areas which are shown on the right, together with earthquakes distribution and main tectonic elements.

B_0, and the Extinction Length, Le, given by:

$$B_0 = \frac{\eta_s}{\eta_i + \eta_s} = \frac{Q_s^{-1}}{Q_i^{-1} + Q_s^{-1}};\ Le^{-1} = \eta_s + \eta_i$$
$$= \frac{v}{2\pi f}\left(Q_i^{-1} + Q_s^{-1}\right). \quad (1)$$

It is based on the measurement of the seismic wave energy in three consecutive time windows on the seismogram, starting from the *S*-wave onset. In this paper, we use an approach slightly different from the ordinary MLTWA commonly applied in literature, using Fourier Transform instead of Filtering and Averaging technique. In Appendix A the method is described in detail.

Widely used in short period earthquake seismology (see e.g. Sato *et al.* 2012 and the references in this Introduction) MLTWA has also been applied to underground mines data sets (Feustel *et al.* 1996), while similar approaches have been applied to lab data in ultrasonic acoustics (Wei & Fu 2014).

DATA ANALYSIS AND RESULTS

We selected from the INGV-Catalogue (Alparone *et al.* 2015; Gruppo Analisi Dati Sismici 2019) about 5000 local earthquakes with magnitude spanning from 1.5 and 4.8 occurred in the period 2006–2017 and recorded by the seismic permanent network run by Istituto Nazionale di Geofisica e Vulcanologia (INGV-OE; Fig. 1). The seismic network consists of about 80 digital stations equipped with three components Nanometrics Trillium broad-band (40 s) seismometers. The signals are digitized at 100 samples s^{-1} with 24-bit resolution at each station. Earthquake sources within a radius of 100 km from each station and a maximum depth of 20 km

were then extracted. Their sources include both the tectonically (Peloritani Mountains and Hyblean Plateau) and volcanically active (Aeolian Islands and Mt Etna) areas of eastern Sicily. Seismograms were carefully inspected to ensure a good quality of the data on the N–S an E–W horizontal components (absence of spikes, telemetry gaps and multiple signals in the coda, average signal-to-noise ratio greater than 5 in a 15 s long time window starting at 60 s from the origin time). About 11 000 two horizontal components waveforms were considered for the application of MLTWA (see also Appendix A). We selected four frequency bands, centred at a frequency *fc* equal to 1.5, 3, 6 and 12 Hz. *tc* (see definition in Appendix A) was set at 45 s measured from the origin time of each earthquake.

The fit of the observed data to the theoretical ET eq. (A1) was carried out using a grid search method in the parameters space with B_0 spanning from 0.05 to 0.95 with steps of 0.05 and Le^{-1} from 0.005 to 0.12 with steps of 0.005. The sum of least squares residuals was normalized for the minimum values, following the procedure described by Mayeda *et al.* (1992). Uncertainties were estimated calculating the area in the B_0 and Le^{-1} coordinates representing the normalized squared residuals which are not statistically different at a 90 per cent confidence level, thus representing the uncertainty area associated with the estimates at the same confidence level. Other examples of the application of this kind of error estimation are also described in Del Pezzo & Bianco (2010b), where a Mathematica™ code for the entire procedure is also illustrated. The fit thus obtained was also checked using the internal Mathematica™ routine 'FindMinimum', using the Conjugate Gradient method instead of Grid Search. Results are comparable inside the uncertainty.

In Fig. 2 we show the data distribution in the source–receiver distance range 0–50 km. Distances larger than 50 km were eliminated, due to a possible contamination of the late coda signals with the background noise. As observed in many tectonically active zones investigated with MLTWA (see e.g. Sato *et al.* 2012 and references therein) the Energy in the time windows closest to the *S*-wave arrivals show the largest scatter as a function of distance, while the scatter decreases in the following energy windows. This phenomenon is explained as a radiation pattern effect, which is still visible in the coda waves following the ballistic *S* waves, while it disappears in the late coda.

Panel (a) (Etna) of Fig. 2 shows that at lowest frequency (1–2 Hz), in the distance interval from 5 to 7 km, the best fit theoretical model overestimates the experimental normalized energy. This effect is also present, but much less marked, in the 1–2 Hz data of panel (b) (Eolie). We checked anyway that it does not severely affect the average estimate of B_0 and Le^{-1} neither in zone (a) nor in (b). We explain this effect as due to the extremely heterogeneous crustal structure towards the surface. Seismograms from receivers close to the source (hypocentral distance less than 7 km) record less energy in the time window starting from *S* waves onset than those from more distant receivers, as in a pure diffusive regime. The energy (apparently) lost at short distance is recovered in the second and third windows. This effect is more evident at Etna than at the other zones investigated, where much less short distance data are available and/or the heterogeneity at surface is smaller.

In Table 1 the estimates of B_0 and Le^{-1} together with correspondent Q_s^{-1} the inverse scattering quality factor, Q_i^{-1}, the inverse intrinsic quality factor and their sum Q_t^{-1}, the inverse total quality factor, are reported for the frequency bands investigated.

For each subzone taken into consideration, we report in Fig. 3 the pattern of Q_i^{-1}, Q_s^{-1} and Q_t^{-1} versus frequency. Experimental data were fit to the power-law $Q = Q_0(f/f_0)^n$ with $f_0 = 1$ Hz (Table 2).

The estimated values correspond to a half-space earth model. As the half-space model is an approximate (rough) assumption, we investigated how the effects of a more realistic earth model would affect the estimates already obtained in the half-space assumption. To do this we applied the method described by Del Pezzo & Bianco (2010a). In Appendix B, we report only a brief synthesis of this method. Details are widely described in Del Pezzo & Bianco (2010a).

Results from this check indicate that the parameters B_0 and Le^{-1}, calculated in a half-space assumption are overestimated due to the effect of the decreasing heterogeneity in the mantle as compared with that in the crust. We wish to remark here that the results 'corrected' for a scattering crust overlying a transparent mantle indicate the order of magnitude and are not precise estimates of the values which actually characterize the scattering crust. In some cases the overestimation of Le^{-1} is unreasonably as high as a factor 8. This effect is due to the gross approximations of the method (see Appendix B) which yields very unstable results at the extreme values of the grid search. It is not our aim here, however, to give precise estimates of the actual attenuation parameters, which may be the goal of future attempts, but only a check of the real existence of such a bias. Pisconti *et al.* (2015) tried to directly fit the coda Energy Envelopes recorded in Central Italy to those numerically calculated (using the method developed by Yoshimoto 2000) assuming different B_0 and Le^{-1} values in three different crustal model, all overlying a transparent mantle. They obtained more precise and reasonable results, all of which confirming a real overestimation of a factor 3–4.

In Fig. 4 we plot the corrected together with the original estimates of B_0 and Le^{-1} as a function of frequency for each area. Note that in few cases, due to the intrinsic instability of the procedure, corrections could not be applied (see Del Pezzo *et al.* 2011).

DISCUSSION

In this work, we investigated on the mechanisms of attenuation of *S* waves in the crust of eastern Sicily measuring the relative contributions of intrinsic absorption and scattering attenuation to the total attenuation. Due to the marked heterogeneity of the geological structure of Eastern Sicily we applied MLTWA separately in different sectors of the study area selected on the base of local homogeneity in the tectonic regime. We thus divided the Eastern Sicily in four sectors: Mt Etna, Aeolian Islands, Peloritani Mountains and Hyblean Plateau (Fig. 1). The first two sectors are sites of active volcanism, the other two are seismically active, non-volcanic areas.

Results show that there are nearly uniform seismic attenuation properties in the two zones characterized by active volcanism (Mt Etna and Aeolian Islands). Analogously, the non-volcanic active regions of Hyblean Plateau and Peloritani Mountains share a similar attenuation pattern. In particular, the two volcanic sectors show a predominance of scattering mechanism in the seismic energy attenuation for frequencies up to 6 Hz, indicating that the geological heterogeneity in volcanoes (magma intrusions, sources of heat flow, faults oriented in different directions, strong layering—see Supporting Information) play the most important role in redistributing the seismic energy lost by the primary waves into the seismic coda. On the contrary, in the two adjacent seismically active non-volcanic regions, intrinsic dissipation is predominant.

Results for each geodynamic domain are summarized in the next subsections.

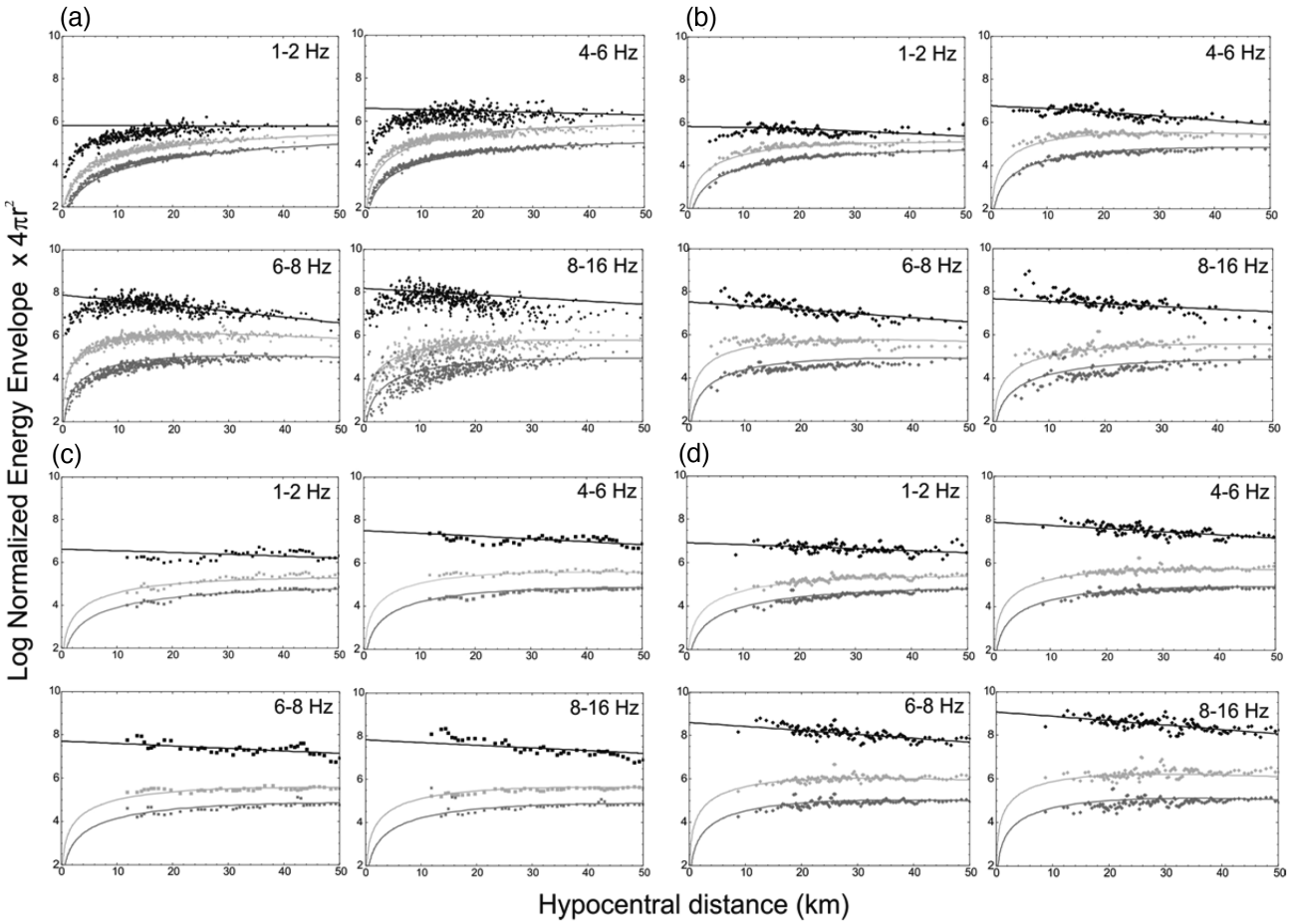

Figure 2. Normalized energy plots at each area and frequency band, corrected for the geometrical spreading factor. Black, light grey and dark grey represent 0–12, 12–24 and 24–36 s windows used for the energy measurements. The best estimate of B_0 and Le^{-1} are obtained from the best fits indicated as solid black lines. (a) Etna; (b) Aeolian Islands; (c) Hyblean Plateau and (d) Peloritani Mountains.

Table 1. Measured B_0–Le^{-1} and $B_{0\mathrm{Corr}}$–$Le^{-1}{}_{\mathrm{Corr}}$ couples and corresponding quality factors, for each study region.

	F	B_0	Le^{-1}	Q_s	Q_i	Q_t	$B_{0\mathrm{corr}}$	$Le_{\mathrm{corr}}{}^{-1}$	$Q_{s\mathrm{corr}}$	$Q_{i\mathrm{corr}}$	$Q_{t\mathrm{corr}}$
AEOLIAN I.	**1.5**	0.8	0.076	44	177	35	0.7	0.032	113	330	84
	3	0.7	0.092	84	195	59	0.6	0.046	195	292	117
	6	0.5	0.060	359	359	179	0.3	0.026	1225	611	408
	12	0.3	0.036	1994	854	598	0.1	/	/	/	/
PELORITANI	**1.5**	0.5	0.036	166	136	75	0.3	0.009	1055	382	280
	3	0.3	0.044	408	175	122	0.1	0.02	2491	299	269
	6	0.2	0.048	1121	280	224	/	/	/	/	/
	12	0.2	0.052	2760	487	414	/	/	/	/	/
ETNA	**1.5**	0.8	0.064	56	168	42	0.7	0.024	165	345	112
	3	0.7	0.076	109	202	71	0.5	0.035	285	334	154
	6	0.6	0.088	222	272	122	0.4	0.046	583	391	234
	12	0.2	0.032	3364	841	673	/	/	/	/	/
HYBLEAN P.	**1.5**	0.5	0.036	150	150	75	0.3	0.009	1043	470	313
	3	0.4	0.040	384	207	135	0.2	0.008	1830	420	366
	6	0.2	0.028	1922	481	384	/	/	/	/	/
	12	0.3	0.036	2392	797	598	0.1	/	/	/	/

Volcanic domains of Mt Etna and Aeolian Islands

In both domains we observe that *Le* ranges between *ca*. 60 and 90 km and the value of the seismic albedo B_0 is higher than 0.5 below 6 Hz and decreases systematically with frequency (Table 1) indicating that, at low frequency, scattering attenuation dominates over intrinsic absorption (Fig. 3). At higher frequency, intrinsic attenuation prevails over scattering. Q_i, Q_s and Q_t show a strong frequency dependence of the type $Q = Q_0(f/f_0)^n$, with f_0 reference frequency set at 1 Hz and n ranging from 0.7 to 1.9 (Table 2). The frequency dependence of Q_s is stronger than that of Q_i in both regions. According to several authors (see e.g. Sato *et al.* 2012), it can be considered as dependent on the average scale dimension

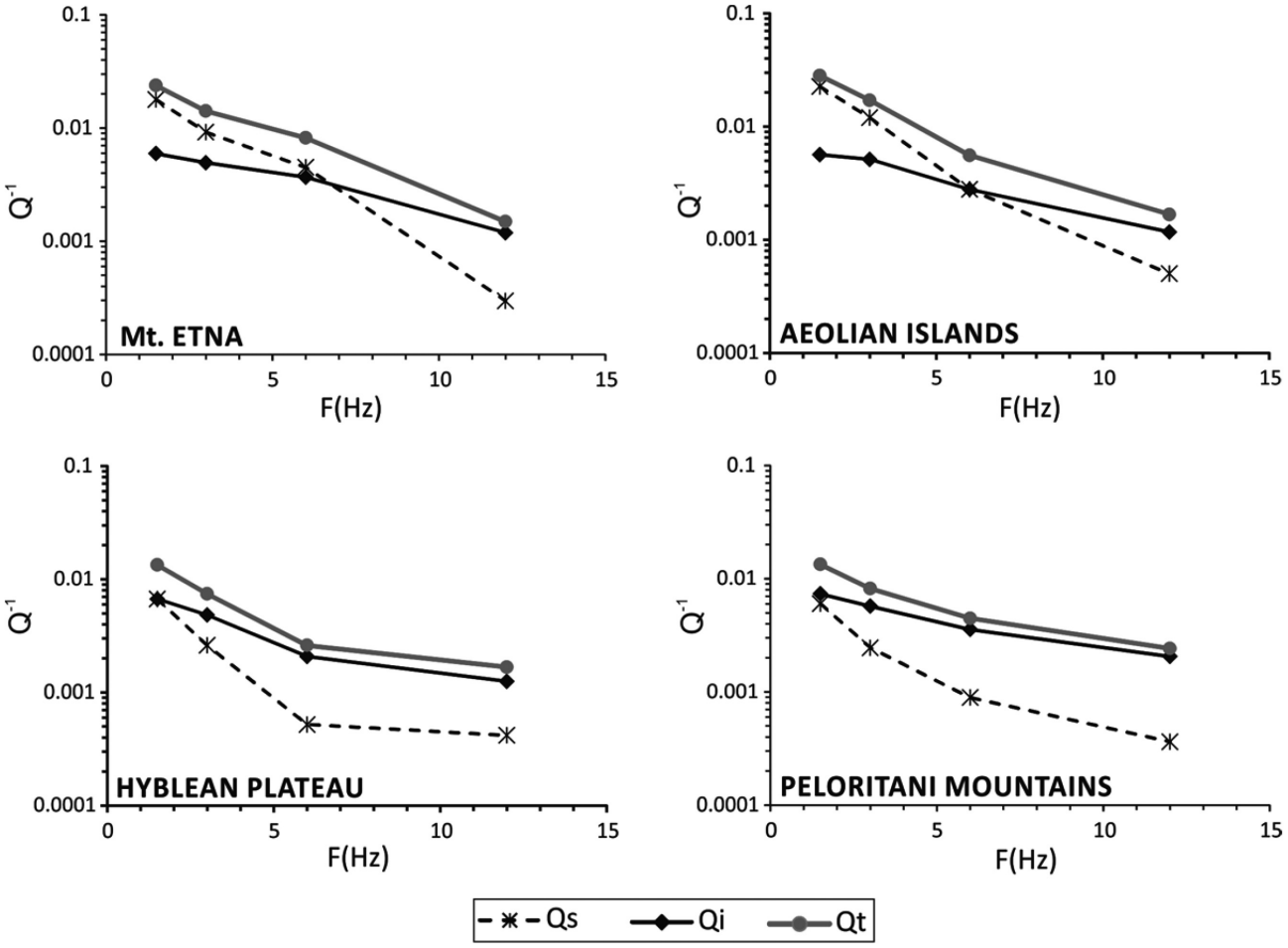

Figure 3. Pattern of Q_i^{-1}, Q_s^{-1} and Q_t^{-1} versus frequency for each study area.

Table 2. Attenuation laws estimated for Q_i, Q_s and Q_t in each study area.

REGION	$Q_i = (Q_0 \pm \sigma)(f/f_0)^{n \pm \sigma}$	$Q_s = (Q_0 \pm \sigma)(f/f_0)^{n \pm \sigma}$	$Q_t = (Q_0 \pm \sigma)(f/f_0)^{n \pm \sigma}$
AEOLIAN I.	$Q_i = (105 \pm 1)f^{0.8 \pm 0.2}$	$Q_s = (15 \pm 2)f^{1.9 \pm 0.3}$	$Q_t = (16 \pm 1)f^{1.4 \pm 0.2}$
PELORITANI	$Q_i = (97 \pm 1)f^{0.6 \pm 0.1}$	$Q_s = (94 \pm 1)f^{1.4 \pm 0.1}$	$Q_t = (52 \pm 1)f^{0.8 \pm 0.1}$
ETNA	$Q_i = (102 \pm 1)f^{0.7 \pm 0.2}$	$Q_s = (17 \pm 2)f^{1.9 \pm 0.5}$	$Q_t = (20 \pm 2)f^{1.3 \pm 0.3}$
HYBLEAN P.	$Q_i = (97 \pm 1)f^{0.9 \pm 0.1}$	$Q_s = (91 \pm 2)f^{1.4 \pm 0.3}$	$Q_t = (48 \pm 1)f^{1.1 \pm 0.1}$

of Earth heterogeneity (Leary 1995). This significant frequency dependence is observed when the heterogeneities responsible for scattering are of sizes comparable to the lowest frequency analysed (e.g. Mayeda *et al.* 1992; Canas *et al.* 1998; Akinci & Eydôgan 2000; Giampiccolo *et al.* 2006; Tuvè *et al.* 2006; Mukhopadhyay *et al.* 2010).

It is noteworthy that the present results match quite well with the Q estimates obtained for Mt Etna by Del Pezzo *et al.* (2015) based on a much more limited data set, indicating the robustness of the used technique. Results similar to the present ones have been obtained in other volcanoes, such as Mt Merapi (Wegler & Lur 2001) and Mt Vesuvius (Bianco *et al.* 1999; Del Pezzo *et al.* 2016). According to Carcolè & Sato (2010) seismic waves propagating in volcanic regions are strongly scattered by velocity and density fluctuations which are expected to be higher in low velocity regions where fluids, like partially melted magma and/or water, accumulates or flow. The same authors associate intrinsic absorption with the presence of fluids. The predominance of scattering attenuation is in good agreement with results from 3D velocity and attenuation tomography, which show the presence of many zones with velocity (both P and S wave) and attenuation contrasts in the upper crust (Patanè *et al.* 2002; Barberi *et al.* 2004; De Gori *et al.* 2005; Martinez Arevalo *et al.* 2005; Patanè *et al.* 2006; De Gori *et al.* 2011; Alparone *et al.* 2012). The main structural feature enlightened by all the above cited studies is a HVB (high velocity body) extending between 2 and 7 km b.s.l. (Patanè *et al.* 2006). Other two significant features were imaged by a recent joint active and passive P-wave tomography performed in northeastern Sicily, including Mt Etna and Aeolian Islands (Dìaz-Moreno *et al.* 2018), carried out in the frame of TOMO-ETNA field project (Ibáñez *et al.* 2016). The first one is a high P-wave velocity body oriented NE–SW and located under the southeastern sector of the volcano, between 4 and 14 km below the sea level; the second one is a low P-wave velocity located to the west of the central craters.

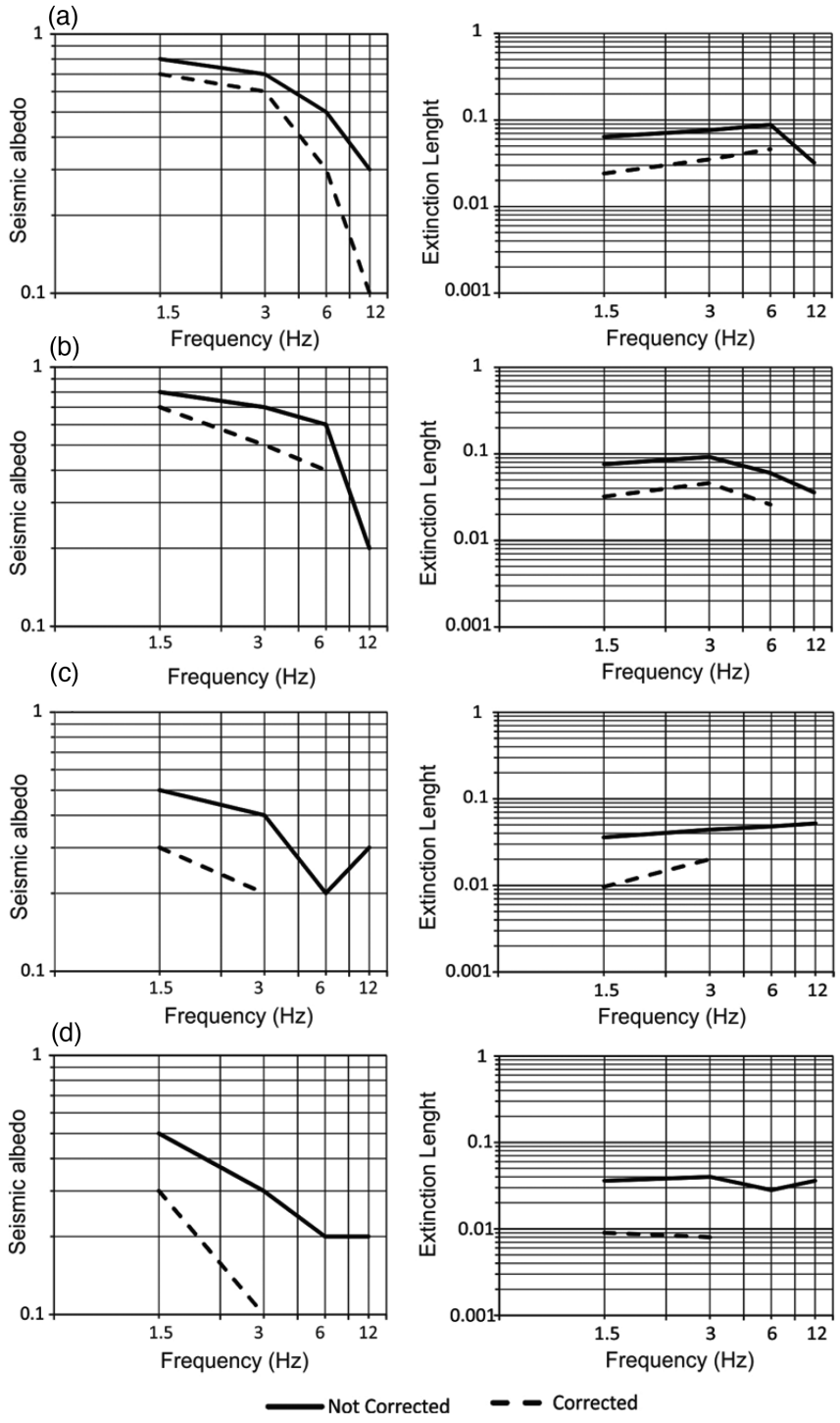

Figure 4. Seismic albedo and extinction length, as a function of frequency, for each study area: (a) Etna; (b) Aeolian Islands; (c) Hyblean Plateau and (d) Peloritani Mountains.

In the Aeolian Islands the geological heterogeneity presumably generating the scattering attenuation is associated with the arc volcanism and the subduction of tectonic plates. Large lateral velocity variations and sharp velocity contrasts are shown by studies based on 3D seismic tomography (Di Stefano *et al.* 1999; Chiarabba *et al.* 2008; Diaz-Moreno *et al.* 2018). The most significant features are: (1) a low velocity anomaly WNW–ESE oriented, extending from 2 to 14 km b.s.l., between Filicudi and the Vulcano–Lipari complex; (2) a low velocity anomaly NW–SE trending, located between 2 and 8 km b.s.l. in the Gulf of Patti; 3) a low-velocity anomaly extending beneath Panarea and Stromboli at a depth ranging between 2 and 14 km which, according to several authors (Piromallo & Morelli 2003; Montuori *et al.* 2007; Chiarabba *et al.* 2008; Caló *et al.* 2009; Scarfì *et al.* 2016), represents the probable location of magma accumulation beneath such Tyrrhenian volcanoes.

Tectonic domains of Peloritani Mountains (Northeastern Sicily) and Hyblean Plateau (Southeastern Sicily)

In the region of Peloritani Mountains B_0 decreases with frequency and its value is lower or equal to 0.5 at all frequencies, indicating a predominance of intrinsic dissipation. *Le* slightly increases with frequency and varies from 36 to 52 km. Similarly, the Hyblean Plateau shows that B_0 is below 0.5. *Le* slightly increases until 3 Hz, decreases between 3 and 6 Hz and then it increases again. Its value ranges between 28 and 40 km. Intrinsic attenuation prevails over scattering except at 1.5 Hz where Q_i and Q_s are comparable. Q_t is close to Q_i in the whole frequency range investigated (Fig. 3). Interestingly, Giampiccolo & Tuvè (2018) found that Q-coda (Q_c) measured in the Peloritani Mountains region using almost the same data set follows the empirical relationship $Q_c = (50 \pm 1)(f/f_0)^{(0.7\pm0.1)}$. This pattern is very close to the relation obtained for Q_t in this study (Table 2) and supports the hypothesis that attenuation inferred from the early coda decay tends to be a combination of both intrinsic and scattering attenuation for increasing heterogeneity (i.e. Del Pezzo *et al.* 2016 and references therein). It is on the other hand widely accepted that Q_c estimated fitting the Single scattering model to the late coda envelope (long lapse time) is close to Q_i (Mayor *et al.* 2016). The results of Q_c regionalization (Giampiccolo and Tuvè 2018) evidenced a broad region of low Q_c values in the central-western part of the present zone. The low Q_c values coincide with low V_P and high V_P/V_S volumes found by recent tomography studies (Scarfì *et al.* 2016; Totaro *et al.* 2017), that have been interpreted as due to the presence of fluids filled fractures. According to Giammanco *et al.* (2008), seismic activity which characterizes this sector of the Peloritani region, is compatible with the migration of subcrustal fluids towards the surface through the complex network of tectonic structures in the area. This evidence reinforces the idea that intrinsic absorption is correlated with the presence of fluids (i.e. Carcolè & Sato 2010). The present results are comparable with those obtained by Tuvè *et al.* (2006) who found that scattering attenuation is only slightly larger than intrinsic attenuation at low frequency in the northeastern sector of the Peloritani Mountains, towards the Strait of Messina. The average heterogeneity scale is dependent on the scattering regime (Sato *et al.* 2012) and is related to the size and distribution of geological fractures. At 1.5 Hz, assuming a *S*-wave velocity of 3 km s^{-1} and a scale length of heterogeneity of the same order of the wavelength, we can estimate from the present results an average dimension around 2 km.

For the Hyblean Plateau, Q_t, Q_s and Q_i are, within the errors, comparable with those obtained by Giampiccolo *et al.* (2006). All the attenuation parameters are frequency dependent and the coefficient n ranges between 0.9 and 1.8. As observed for the Peloritani Mountains, independent estimates of Q_c versus frequency (Giampiccolo *et al.* 2002) provided an empirical relationship given by $Q_c = Q_0(f/f_0)^n$, with $f_0 = 1$ Hz, Q_0 ranging from 20 to 70 and n between 0.7 and 1.6, in the lapse time between 10 and 30 s, which is very similar to that of Q_t obtained in the present paper by MLTWA technique (Table 2). Intrinsic absorption predominates over scattering above 1.5 Hz whereas at low frequencies scattering attenuation becomes important (Fig. 3). Our results evidence a weakly heterogeneous crust in the Hyblean Plateau which well correlates with the tectonic characteristics of the area, basically characterized by large scale heterogeneities (e.g. Bianca *et al.* 1999; Azzaro & Barbano 2000; de Lorenzo *et al.* 2004; Musumeci *et al.* 2005), as also supported by 3D local tomography studies (i.e. Scarfì *et al.* 2007; Brancato *et al.* 2009; Musumeci *et al.* 2014; Giampiccolo *et al.* 2017). On the other hand, a recent interpretation (Giampiccolo *et al.* 2017), jointly based on velocity and attenuation tomography, allowed to identify several volumes characterized by high fluid content, which can be related both to the strong intrinsic attenuation and to the distribution of seismicity. In particular, according to the authors, the presence of fluids in the crust weakens the rocks and controls the background seismicity, which is characterized by earthquakes whose magnitude M_L rarely exceeds 3.5, source radii between 100 and 500 m and very low stress-drop values ranging from 0.1 to 10 bar (de Lorenzo *et al.* 2004; Tusa *et al.* 2006).

CONCLUSIONS

This study provides a reappraisal of the attenuation parameters for the shear waves in Eastern Sicily and adds new information on the sector of Aeolian Islands. The attenuation pattern of different seismic domains indicates that, at low frequencies (below 6 Hz), scattering is the main attenuation mechanism in volcanic areas whereas tectonic regions are characterized by the predominance of intrinsic absorption. Above 6 Hz intrinsic attenuation prevails over scattering in all the investigated regions. Q_t is found to be strongly frequency dependent in the whole Eastern Sicily, the value of the coefficient n being higher than 0.7 (Table 2). As a consequence, the total attenuation of seismic waves at high frequencies is less pronounced than at low frequencies, a pattern which is peculiar for the majority of the tectonically active areas investigated using the MLTWA technique in similar distance and frequency ranges. In Fig. 5 we plot, the present estimates of B_0 and Le^{-1} as a function of frequency together with those taken from literature worldwide and averaged, separately, for volcanic and tectonic areas (Mayeda *et al.* 1992; Jin *et al.* 1994; Akinci *et al.* 1995; Tselentis 1998; Ugalde *et al.* 1998, 2007; Akinci & Eydôgan 2000; Bianco *et al.* 2002, 2005; Dutta *et al.* 2004; Goutbeek *et al.* 2004; Vargas *et al.* 2004; Abubakirov 2005; Bindi *et al.* 2006, 2009; Giampiccolo *et al.* 2006; Tuvè *et al.* 2006; Lemzikov, 2007, 2008; Sahin *et al.* 2007; Chung *et al.* 2009; Yoshimoto & Okada 2009; Lee *et al.* 2010; Mukhopadhyay & Sharma 2010 2010; Del Pezzo *et al.* 2011; Meirova & Pinski 2014; Sawazaki & Enescu 2014). Interestingly, our results are inside the 1σ uncertainty level associated with the world average. Fig. 6 shows the comparison of the present Q_s^{-1} and Q_i^{-1} estimates (calculated from B_0 and Le^{-1} using eq. 1) with those from other zones investigated through MLTWA. We observe that scattering attenuation is higher than the majority of the tectonically active areas, and it is similar to the values measured in Messina Strait (Tuvè *et al.* 2006), West Greece (Tselentis 1998), Southern Spain (Akinci *et al.* 1995), North Anatolia (Akinci & Eydôgan 2000), Iwate (Sawazaki & Enescu 2014) and Central California (Mayeda *et al.* 1992). The frequency pattern of the intrinsic absorption is similar to that generally observed in other tectonic domains. Mt Etna and Aeolian Islands show scattering attenuation at low frequencies close to that of many other volcanic areas, whereas it is stronger and of the same order of that observed in the crust of Andes (Badi *et al.* 2009) and at Klyuchevskoy Volcano (Lemzikov 2008) in the frequency bands above 6 Hz. The above considerations are based on the hypothesis of a uniform Earth model. It is worth stressing that, by applying the corrections for an opaque crust over a transparent mantle suggested by Del Pezzo & Bianco (2010a) we find that, at all frequencies and in each study area, both B_0 and Le^{-1} are lower than the values estimated under the assumption of a uniform model. For Mt Etna and Aeolian Islands the difference between non-corrected and corrected estimates is not significant (Fig. 4; Table 1). As also observed by Del Pezzo *et al.* (2011) this happens when scattering

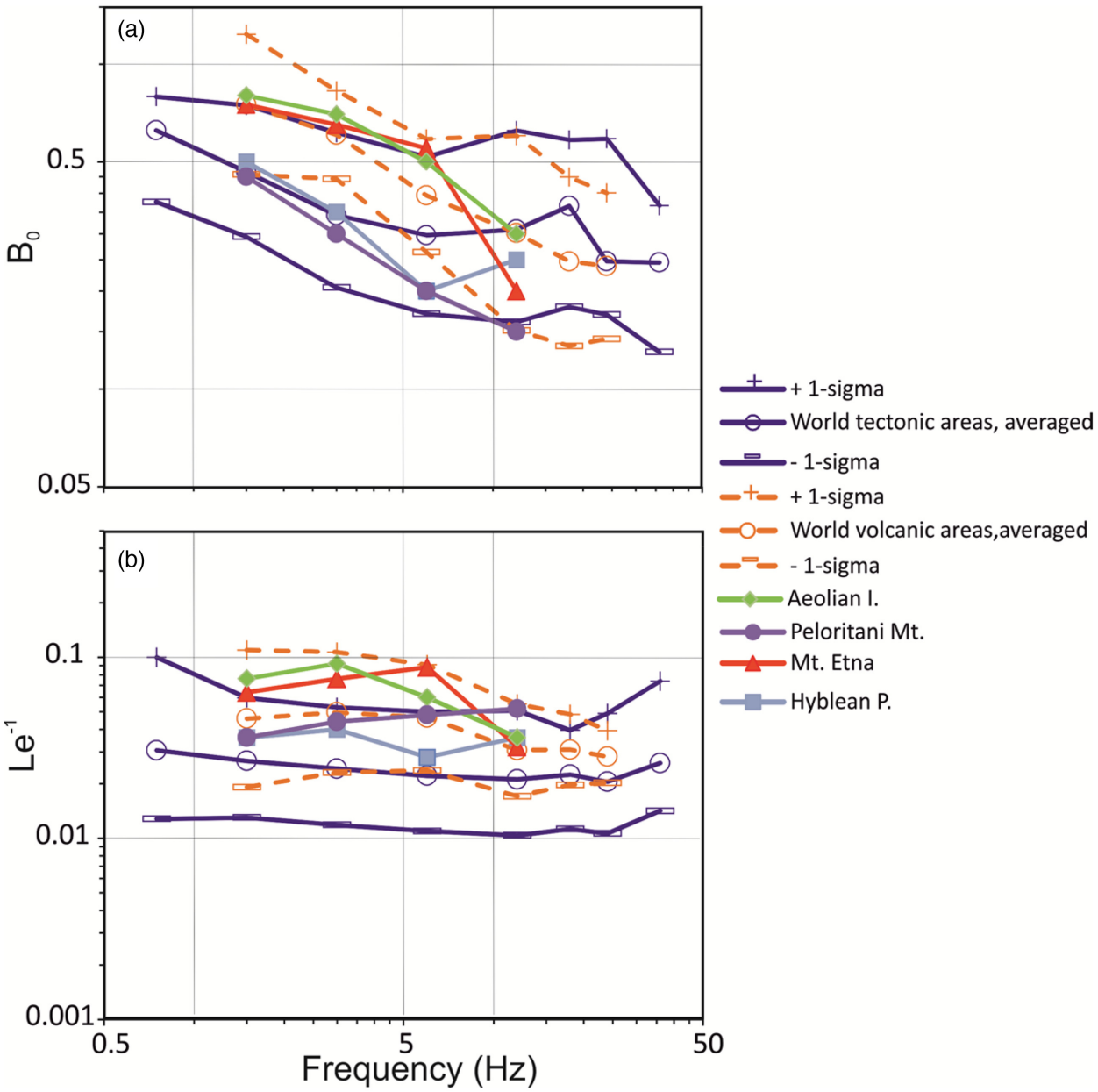

Figure 5. Comparison of B_0 (a) and Le^{-1} (b) estimated in this study, with those obtained worldwide and averaged separately for volcanic and tectonic areas. 1σ standard deviation is also plotted above and below each average value.

is strongly dominant (Del Pezzo & Bianco 2010a). Differences are more important for the zones of Peloritani Mountains and Hyblean Plateau.

The effect of an opaque crust overlying a transparent mantle was discussed by Margerin *et al.* (1999), who were the first to demonstrate how much energy is lost when transmitted into the mantle (energy leakage), which, being transparent, does not transmit back energy by scattering to the receiver. This crust–mantle leakage would produce in the same way an overestimation of the attenuation parameters when estimated in the half-space assumption. In addition, as also numerically observed by Yoshimoto (2000) and by other authors in their applications to different areas (i.e. Hoshiba *et al.* 2001; Bianco *et al.* 2005; Del Pezzo & Bianco 2010a; Del Pezzo *et al.* 2011), in the case of uniform half-space assumption the total attenuation results always overestimated. As already discussed above, the precise amount of this overestimation in the present case cannot be estimated, due to the approximations in the methodology which leads to large uncertainties. These last are maxima at the borders of the B_0–Le^{-1} grid of values used by Del Pezzo and Bianco (2010a) to obtain the correction nomogram used in the present and in other applications (see e.g. Del Pezzo *et al.* 2011). Interesting is however the difference between the half-space estimates and the 'corrected' estimates in the four zone considered in this paper. These differences, despite qualitative, are interpreted as indicative of different tectonic properties.

The above considerations should be always taken into account for the definition of the attenuation laws for the seismic hazard purposes (Del Pezzo *et al.* 2015).

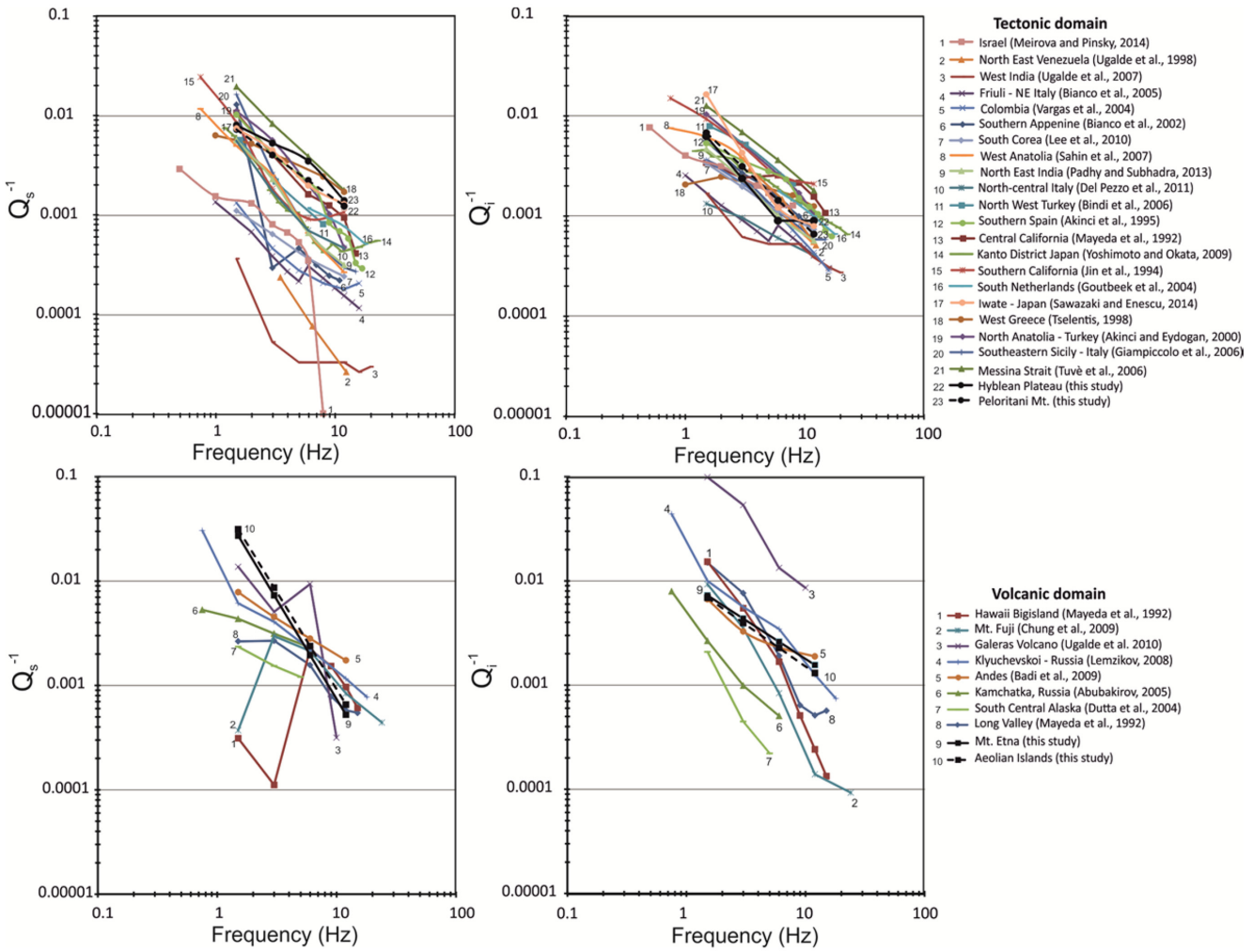

Figure 6. Worldwide estimates of Q_s^{-1} and Q_i^{-1}, including those obtained in this study.

The results obtained in this paper complete the information on the seismic attenuation mechanisms in Eastern Sicily, aimed at improving the formulation of reliable seismic hazard maps for this zone.

ACKNOWLEDGEMENTS

We are grateful to the Editor, to Ludovic Margerin and to the anonymous reviewer for the accurate reading of the manuscript and for their constructive criticism and suggestions which helped us to improve the organization of the paper. This work has been partially supported by the Spanish project KNOWAVES from the Spanish Ministry of Science and Technology.

REFERENCES

Abubakirov, I.R., 2005. Attenuation characteristics of transverse waves in the lithosphere of Kamchatka estimated from observations at the Petropavlovsk digital broadband station, *Izv. Phys. Solid Earth.,* **41**(10), 813–824.

Akinci, A., Del Pezzo, E. & Ibáñez, J., 1995. Separation of scattering and intrinsic attenuation in Southern Spain and western Anatolia (Turkey), *Geophys. J. Int.,* **121,** 337–353.

Akinci, A. & Eyidôgan, H., 2000. Scattering and anelastic attenuation of seismic energy in the vicinity of north Anatolian fault zone, eastern Turkey, *Phys. Earth planet. Inter.,* **122,** 229–239.

Alparone, S., Barberi, G., Cocina, O., Giampiccolo, E., Musumeci, C. & Patanè, D., 2012. Intrusive mechanism of the 2008–2009 Mt. Etna eruption: Constraints by tomographic images and stress tensor analysis, *J. Volc. Geotherm. Res.,* **229–230,** 50–63.

Alparone, S., Maiolino V., Mostaccio A., Scaltrito A., Ursino A., Barberi G., Di Grazia G., Giampiccolo E., Musumeci C., Scarfì L., Zuccarello L., 2015. Instrumental seismic catalogue of Mt. Etna earthquakes (Sicily, Italy): ten years (2000-2010) of instrumental recordings, *Ann. Geophys,* **58**(4), S0435, doi:10.4401/ag-6591.

Azzaro, R. & Barbano, M.S., 2000. Analysys of the seismicity of southeastern Sicily: a proposed tectonic interpretation, *Ann. Geophys.,* **43,** 171–188.

Azzaro, R., Bernardini, F., Camassi, R. & Castelli, V., 2007. The 1780 seismic sequence in NE Sicily (Italy): shifting an underestimated and mislocated earthquake to a seismically low rate zone, *Nat. Hazards,* **42,** 149–167.

Badi, G., Del Pezzo, E., Ibáñez, J.M., Bianco, F., Sabbione, N. & Araujo, M., 2009. Depth dependent seismic scattering attenuation in the Nuevo Cuyo region (southerncentral Andes), *Geophys. Res. Lett.,* **36**(24), L24307. http://dx.doi.org/10.1029/2009GL041081

Barberi, G., Cosentino, M.T., Gervasi, A., Guerra, I., Neri, G. & Orecchio, B., 2004. Crustal seismic tomography in the Calabrian Arc region, south Italy, *Phys. Earth planet. Inter.,* **147,** 297–314.

Bianca, M., Monaco, C., Tortorici, L. & Cernobori, L., 1999. Quaternary normal faulting in southeastern Sicily (Italy): a seismic source for the 1693 large earthquake, *Geophys. J. Int.,* **139,** 370–394.

Bianco, F., Castellano, M., Del Pezzo, E. & Ibáñez, J.M., 1999. Attenuation of short period seismic waves at Mt. Vesuvius, Italy, *Geophys J. Int.,* **138**(1), 67–76.

Bianco, F., Del Pezzo, E., Castellano, M., Ibáñez, J. & Di Luccio, F., 2002. Separation of intrinsic and scattering seismic attenuation in the Southern Apennine zone, Italy, *Geophys. J. Int.,* **150,** 10–22.

Bianco, F., Del Pezzo, E., Malagnini, L., Di Luccio, F. & Akinci, A., 2005. Separation of depth-dependent intrinsic and scattering seismic attenuation in the northeastern sector of the Italian Peninsula, *Geophys. J. Int.,* **161,** 130–142.

Bindi, D., Parolai, S., Grosser, H., Milkereit, C. & Karakisa, S., 2006. Crustal attenuation characteristics in Northwestern Turkey in the range from 1 to 10 Hz, *Bull. seism. Soc. Am.,* **96,** 200–214.

Brancato, A., Hole, J.A., Gresta, S. & Beale, J.N., 2009. Determination of seismogenic structures in southeastern Sicily (Italy) by high-precision relative relocation of microearthquakes, *Bull. seism. Soc. Am.,* **99,** 1921–1936.

Calò, M., Dorbath, C., Luzio, D., Rotolo, S.G. & D'Anna, G., 2009. Local earthquakes tomography in the southern Tyrrhenian region: geophysical and petrological inferences on subducting lithosphere, in *Subduction Zone Geodynamics, Frontiers in Earth Sciences,* eds Lallemand, S. & Funiciello, F., Springer-Verlag. doi:10.1007/978-3-540-87974-9.

Canas, J.A., Ugalde, A., Pujades, L.G., Carracedo, J.C., Blonco, M.J. & Soler, V., 1998. Intrinsic and scattering seismic wave attenuation in the Canary Islands, *J. geophys. Res.,* **103,** 15 037–15 049.

Carcolé, E. & Sato, H., 2010. Spatial distribution of scattering loss and intrinsic absorption of short-period S waves in the lithosphere of Japan on the basis of the Multiple Lapse Time Window Analysis of Hi-net data, *Geophys. J. Int.,* **180**(1), 268–290.

Cavazza, W. & Wezel, F.C., 2003. The Mediterranean region—a geological primer, *Episodes,* **26,** 160–168.

Chiarabba, C., De Gori, P. & Speranza, F., 2008. The southern Tyrrhenian subduction zone. Deep geometry, magmatism and Plio-Pleistocen evolution, *Earth planet. Sci. Lett.,* **268,** 408–423.

Chung, T.W., Lees, J.M., Yoshimoto, K., Fujita, E. & Ukawa, M., 2009. Intrinsic and scattering attenuation of the Mt Fuji region, Japan, *Geophys. J. Int.,* **177,** 1366–1382.

De Gori, P., Chiarabba, C. & Patanè, D., 2005. Qp structure of Mount Etna: constraints for the physics of the plumbing system, *J. geophys. Res.,* **110**(B05303), doi:10.1029/2003JB002875.

De Gori, P., Chiarabba, C., Giampiccolo, E., Martinez-Arèvalo, C. & Patanè, D., 2011. Body wave attenuation heralds incoming eruptions at Mt. Etna, *Geology,* **39,** 503–506.

De Guidi, G., Imposa, S., Scudero, S. & Palano, M., 2014. New evidence for Late Quaternary deformation of the substratum of Mt. Etna volcano (Sicily, Italy): clues indicate active crustal doming, *Bull. Volcanol.,* **76,** 816,.

de Lorenzo, S., Di Grazia, G., Giampiccolo, E., Gresta, S., Langer, H., Tusa, G. & Ursino, A., 2004. Source and Qp parameters from pulse width inversion of microearthquake data in southeastern Sicily, Italy, *J. geophys. Res.,* **109**.

De Luca, G., Filippi, L., Caccamo, D., Neri, G. & Scarpa, R., 1997. Crustal structure and seismicity of Southern Tyrrhenian basin, *Phys. Earth planet. Inter.,* **103,** 117–133.

Del Pezzo, E. & Bianco, F., 2010a. Two-layer earth model corrections to the MLTWA estimates of intrinsic- and scattering-attenuation obtained in a uniform half-space, *Geophys. J. Int.,* **182**(2), 949–955.

Del Pezzo, E. & Bianco, F., 2010b. MathLTWA: Multiple lapse time window analysis using Wolfram Mathematica e7, *Comput. Geosci.,* **36**(10), 1388–1392.

Del Pezzo, E., Bianco, F., Marzorati, S., Augliera, P., D'Alema, E. & Massa, M., 2011. Depth-dependent intrinsic and scattering seismic attenuation in north central Italy, *Geophys. J. Int.,* **186**(1), 373–381.

Del Pezzo, E., Bianco, F., Giampiccolo, E., Tusa, G. & Tuvè, T., 2015. A reappraisal of seismic Q evaluated at Mt. Etna volcano. Receipt for the application to risk analysis, *J. Seismol.,* **19**(1), 105–119.

Del Pezzo, E., Ibáñez, J., Prudencio, J., Bianco, F. & De Siena, L., 2016. Absorption and Scattering 2D Volcano Images from Numerically Calculated Space-weighting functions, *Geophys. J. Int.,* **206,** 742–756.

Díaz-Moreno, A., Barberi G., Cocina O., Koulakov I., Scarfì L., Zuccarello L., Prudencio J., Garcia-Yeguas A., Alvarez I., Garcia L., Ibàñez J.M. 2018. New insights on Mt. Etna's Crust and relationship with the regional tectonic framework from joint active and passive P-Wave seismic tomography, *Surv. Geophys.,* **39**(1), 57–97.

Di Stefano, R., Chiarabba, C., Lucente, F. & Amato, A., 1999. Crustal and uppermost mantle structure in Italy from the inversion of P-wave arrival times: geodynamic implications, *Geophys. J. Int.,* **139,** 483–498.

Dutta, U., Biswas, N.N., Adams, D.A. & Papageorgiou, A., 2004. Analysis of S-wave attenuation in South-Central Alaska, *Bull. seism. Soc. Am.,* **94,** 16–28.

Eulenfeld, T. & Wegler, U., 2016. Measurement of intrinsic and scattering attenuation of shear waves in two sedimentary basins and comparison to crystalline sites in Germany, *Geophys. J. Int.,* **205,** 744–757.

Fehler, M., Hoshiba, M., Sato, H. & Obara, K., 1992. Separation of scattering and intrinsic attenuation for the Kanto-Tokai Region, Japan, using measurements of S-wave energy versus hypocentral distance, *Geophys. J. Int.,* **108**(3), 787–800.

Feustel, A.J., Trifu, C.I. & Urbancic, T.I., 1996. Rock-mass characterization using intrinsic and scattering attenuation estimates at frequencies from 400 to 1600 Hz, *Pageoph,* **147**(2), 289–304.

Frankel, A. & Wennerberg, L., 1987. Energy-flux model of seismic coda: separation of scattering and intrinsic attenuation, *Bull. seism. Soc. Am.,* **77,** 1223–1251.

Giammanco, S., Palano, M., Scaltrito, A., Scarfì, L. & Sortino, F., 2008. Possible role of fluid overpressure in the generation of earthquake swarms in active tectonic areas: the case of the Peloritani Mts. (Sicily, Italy), *J. Volc. Geotherm. Res.,* **178,** 795–806.

Giampiccolo, E., Tusa, G., Langer, H. & Gresta, S., 2002. Attenuation in Southeastern Sicily (Italy) by applying different coda methods, *J. Seismol.,* **6**(4), 487–501.

Giampiccolo, E., Gresta, S. & Rasconà, F., 2004. Intrinsic and scattering attenuation from observed seismic codas in Southeastern Sicily (Italy), *Phys. Earth planet. Inter.,* **145**(1-4), 55–66.

Giampiccolo, E., Tuvè, T., Gresta, S. & Patanè, D., 2006. S-waves attenuation and separation of scattering and intrinsic absorption of seismic energy in southeastern Sicily (Italy), *Geophys. J. Int.* **165**(1), 211–222.

Giampiccolo, E., Brancato, A., Manuella, F.C., Carbone, S., Gresta, S. & Scribano, V., 2017. New evidence for the serpentinization of the Palaeozoic basement of southeastern Sicily from joint 3-D seismic velocity and attenuation tomography, *Geophys. J. Int.,* **211,** 1375–1395.

Giampiccolo, E. & Tuvè, T., 2018. Regionalization and dependence of coda Q on frequency and lapse time in the seismically active Peloritani region (northeastern Sicily, Italy), *J. Seismol.,* **22**(4), 1059–1074.

Goutbeek, F.H., Dost, B. & Van Eck, T., 2004. Intrinsic absorption and scattering attenuation in the southern part of the Netherlands, *J. Seismol.,* **8,** 11–23.

Gruppo Analisi Dati Sismici, 2019. 'Catalogo dei terremoti della Sicilia Orientale - Calabria Meridionale (1999-2019)'. Available at: http://www.ct.ingv.it/ufs/analisticatalogolist.php.

Hoshiba, M., Sato, H. & Fehler, M., 1991. Numerical basis of the separation of scattering and intrinsic absorption from full seismogram envelope: a Monte-Carlo simulation of multiple isotropic scattering, *Pap. Meteorol. Geophys.,* **42**(2), 65–91.

Hoshiba, M., Rietbrock, A., Scherbaum, F., Nakahara, H. & Haberland, C., 2001. Scattering attenuation and intrinsic absorption using uniform and depth dependent model—application to full seismogram envelope recorded in Northern Chile, *J. Seismol.,* **5,** 157. https://doi.org/10.1023/A:1011478202750

Ibáñez, J.M. *et al.*, 2016. TOMO-ETNA experiment at Etna volcano: activities on land, *Ann. Geophys.,* **59**(4), S0427. doi: 10.4401/ag-7080.

Jin, A., Mayeda, K., Adams, D. & Aki, K., 1994. Separation of intrinsic and scattering attenuation in southern California using TERRAscope data, *J. geophys. Res.,* **99**(17), 835–17848.

Leary, P.C., 1995. The cause of frequency-dependent seismic absorption in crustal rock, *Geophys. J. Int.,* **122**(1), 143–151

Lee, W.S., Yun, S. & Do, J.Y., 2010. Scattering and intrinsic attenuation of short-period S waves in the Gyeongsang Basin, South Korea, revealed from S-wave seismogram envelopes based on the radiative transfer theory, *Bull. seism. Soc. Am.,* **100**(2), 833–840.

Lemzikov, M.V., 2007. Intrinsic attenuation and scattering of shear waves in the lithosphere of Kamchatka, *J. Volc. Seismol.,* **1**(3), 185–197.

Lemzikov, M.V., 2008. Estimation of shear-wave attenuation characteristics for the Klyuchevskoi volcanic edifice, *J. Volc. Seismol.,* **2,** 108–117.

Margerin, L., Campillo, M., Shapiro, N.M. & van Tiggelen, B., 1999. Residence time of diffuse waves in the crust as a physical interpretation of coda Q: application to seismograms recorded in Mexico, *Geophys. J. Int.,* **138**(2), 343–352.

Martinez-Arèvalo, C., Patanè, D., Rietbrock, A. & Ibáñez, J.M., 2005. The intrusive process leading to the Mt. Etna 2001 flank eruption: constraints from 3-D attenuation tomography, *Geophys. Res. Lett.,* **32,** L21309. doi:10.1029/2005GL023736.

Mauffret, A., 2007. The Northwestern (Maghreb) boundary of the Nubia (Africa) Plate, *Tectonophysics,* **429,** 21–44.

Mayeda, K., Koyanagi, S., Hoshiba, M., Aki, K. & Zeng, Y., 1992. A comparative study of scattering, intrinsic, and coda Q^{-1} for Hawaii, Long Valley and central California between 1.5 and 15 Hz, *J. geophys. Res.,* **97,** 6643–6659.

Mayor, J., Calvet, M., Margerin, L. & Vanderhaeghe, O., 2016. Crustal structure of the Alps as seen by attenuation tomography, *Earth planet. Sci. Lett.,* **439,** 71–80.

McClusky, S., Reilinger, R., Mahmoud, S., Ben Sari, D. & Tealeb, A., 2003. GPS constraints on Africa (Nubia) and Arabia plate motion, *Geophys. J. Int.,* **155,** 126–138.

Meirova, T. & Pinsky, V., 2014. Seismic wave attenuation in Israel region estimated from the multiple lapse time window analysis and S-wave coda decay rate, *Geophys. J. Int.,* **197,** 581–590.

Montuori, C., Cimini, G.B. & Favali, P., 2007. Teleseismic tomography of the southern Tyrrhenian subduction zone: new results from seafloor and land recordings, *J. geophys. Res.,* **112,** 3311.

Mukhopadhyay, S. & Sharma, J., 2010. Attenuation characteristics of Garwhal–Kumaun Himalayas from analysis of coda of local earthquakes, *J. Seismol.,* **14,** 693–713.

Mukhopadhyay, S., Sharma, J., Del Pezzo, E. & Kumar, N., 2010. Study of attenuation mechanism for Garwhal–Kumaun Himalayas from analysis of coda of local earthquakes, *Phys. Earth planet. Inter.,* **180,** 7–15.

Musumeci, C., Patanè, D., Scarfì, L. & Gresta, S., 2005. Stress directions and shear-wave anisotropy: observations from local earthquakes in southeastern Sicily, Italy, *Bull. seism. Soc. Am.,* **95**(4), 1359–1374.

Musumeci, C., Scarfì, L., Palano, M. & Patanè, D., 2014. Foreland segmentation along an active convergent margin: new constraints in southeastern Sicily (Italy) from seismic and geodetic observations, *Tectonophysics,* **630,** 137–149.

Neri, G., Caccamo, D., Cocina, O. & Montalto, A., 1996. Geodynamic implications of earthquake data in the Southern Tyrrhenian Sea, *Tectonophysics,* **258,** 233–249.

Paasschens, J., 1997. Solution of the time-dependent Boltzmann equation, *Phys. Rev.,* **E 56,** 1135–1141.

Padhy, S. & Subhadra, N., 2013. Separation of intrinsic and scattering seismic wave attenuation in Northeast India, *Geophys. J. Int.,* **195**(3), 1892–1903.

Palano, M., Ferranti, L., Monaco, C., Mattia, M., Aloisi, M., Bruno, V., Cannavò, F. & Siligato, G., 2012. GPS velocity and strain fields in Sicily and southern Calabria, Italy: updated geodetic constraints on tectonic block interaction in the central Mediterranean, *J. geophys. Res.,* **117,** doi:10.1029/2012JB009254.

Patanè, D., Chiarabba, C., Cocina, O., De Gori, P., Moretti, M. & Boschi, E., 2002. Tomographic images and 3D earthquake locations of the seismic swarm preceding the 2001 Mt. Etna eruption: Evidence for a dyke intrusion, *Geophys. Res. Lett.,* **29**(10), 1497.

Patanè, D. & Giampiccolo, E., 2004. Faulting processes and earthquake source parameters at Mount Etna: State of the Earth and perspectives, in *Mt. Etna: Volcano Laboratory, Geophys. Monogr. Ser.,* **143,** eds Calvari, S. *et al.*, AGU, doi:10.1029/143GM11

Patanè, D., Barberi, G., Cocina, O., De Gori, P. & Chiarabba, C., 2006. Time-resolved seismic tomography detects magma intrusions at Mount Etna, *Science,* **313,** 821–823,

Piromallo, C. & Morelli, A., 2003. P wave tomography of the mantle under the Alpine-Mediterranean area, *J. geophys. Res.,* **108**(B2), 2065.

Pisconti, A., Del Pezzo, E., Bianco, F. & de Lorenzo, S., 2015. Seismic Q estimates in Umbria Marche (Central Italy): hints for the retrieval of a new attenuation law for seismic risk. *Geophys. J. Int.,* **201**(3), 1370–1382.

Sahin, S., Erduran, M., Alptekin, O. & Cakir, O., 2007. Intrinsic and scattering seismic attenuation in southewestern Anatolia, *Pure appl. Geophys.,* **164,** 2255–2270.

Sato, H. & Fehler, M., 1998. *Seismic Wave Propagation and scattering in the Heterogeneous Earth,* 2nd edn, Vol. **308,** pp. 319, Springer XIV.

Sato, H., Fehler, M. & Maeda, T., 2012. *Seismic wave propagation and scattering in the heterogeneous Earth,* 2nd edn, Springer.

Sawazaki, K. & Enescu, B., 2014. Imaging the high-frequency energy radiation process of a mainshock and its early aftershock sequence: the case of the 2008 Iwate-Miyagi Nairiku earthquake, Japan, *J. geophys. Res.,* **119**(6), 4729–4746.

Scarfì, L., Giampiccolo, E., Musumeci, C., Patanè, D. & Zhang, H., 2007. New insights on 3D crustal structure in southeastern Sicily (Italy) and tectonic implications from an adaptive mesh seismic tomography, *Phys. Earth planet. Inter.,* **161,** 74–85.

Scarfì, L., Barberi, G., Musumeci, C. & Patanè, D., 2016. Seismotectonics of Northeastern Sicily and Southern Calabria (Italy): New constraints on the tectonic structures featuring in a crucial sector for the Central Mediterranean geodynamics, *Tectonics,* **34,** doi:10.1002/2015TC004022.

Sicali, S., Barbano, M.S., D'Amico, S. & Azzaro, R., 2014. Characterization of seismicity at Mt. Etna volcano (Italy) by inter-event time distribution, *J. Volc. Geotherm. Res.,* **270,** 1–9.

Singh, C., Biswas, R., Srijayanthi, G. & Ravi Kumar, M., 2017. Relative role of intrinsic and scattering attenuation beneath the Andaman Islands, India and tectonic implications, *Phys. Earth planet. Inter.,* **271,** 19–28.

Totaro, C., Kukarina, E., Koulakov, I., Neri, G., Orecchio, B. & Presti, D., 2017. Seismotomographic detection of major structural discontinuity in northern Sicily, *Italy, J. Geosci.,* **136**(3), 389–398.

Tselentis, G.A., 1998. Intrinsic and scattering seismic attenuation in W. Greece, *Pure appl. Geophys.,* **153,** 703–712.

Tusa, G., Brancato, A. & Gresta, S., 2006. Source parameters of microearthquakes in southeastern Sicily, Italy, *Bull. seism. Soc. Am.,* **96,** doi:10.1785/0120050071.

Tuvè, T., Bianco, F., Ibanez, J.M., Patanè, D., Del Pezzo, E. & Bottari, A., 2006. Attenuation study in the Straits of Messina area (Southern Italy), *Tectonophysics,* **421,** 173–185.

Ugalde, A., Pujades, L.G., Canas, J.A. & Villasenor, A., 1998. Estimation of the intrinsic absorption and scattering attenuation in northeastern Venezuela (southeastern Carribean) using coda, *Pure appl. Geophys.,* **105,** 685–702.

Ugalde, A., Tripathi, J.N., Hoshiba, M. & Rastogi, B.K., 2007. Intrinsic and scattering attenuation in western India from aftershocks of the 26 January, 2001 Kachchh earthquake, *Tectonophysics,* **429**(1-2), 111–123.

Vargas, C.A., Ugalde, A., Pujades, L.G. & Canas, J.A., 2004. Spatial variation of coda wave attenuation in northwestern Columbia, *Geophys. J. Int.,* **158,** 609–624.

Wegler, U. & Luhr, B.G., 2001. Scattering behaviour at Merapi volcano (Java) revealed from an active seismic experiment, *Geophys. J. Int.,* **145,** 579–592.

Wei, W. & Fu, L.Y., 2014. Monte Carlo simulation of stress-associated scattering attenuation from laboratory ultrasonic measurements. *Bull. seism. Soc. Am.,* **104**(2), 931–943.

Wennerberg, L., 1993. Multiple-scattering interpretations of coda-Q measurements, *Bull. seism. Soc. Am.,* **83**(1), 279–290.

Wu, R.S., 1985. Multiple scattering and energy transfer of seismic waves – separation of scattering effect from intrinsic attenuation – 1. Theoretical modeling Geophys. *J. R. astron. Soc.,* **82,** 57–80.

Yoshimoto, K., 2000. Monte Carlo simulation of seismogram envelopes in scattering media, *J. geophys. Res.,* **105,** 6153–6161.
Yoshimoto, K. & Okada, M., 2009. Frequency-dependent attenuation of S-waves in the Kanto region Japan, *Earth Planets Space,* **61,** 1067–1075.

SUPPORTING INFORMATION

Supplementary data are available at *GJI* online.
supplementary_materials.pdf
Please note: Oxford University Press is not responsible for the content or functionality of any supporting materials supplied by the authors. Any queries (other than missing material) should be directed to the corresponding author for the paper.

APPENDIX A

Energy Envelope $E[r,\ t]$ in ET is given by

$$E\ [r,\ t] \approx \frac{W_0 \exp[-Le^{-1}vt}{4\pi r^2 v}\delta\left[t-\frac{r}{v}\right] + W_0 H\left[t-\frac{r}{v}\right] \times \frac{\left(1-\frac{r^2}{v^2t^2}\right)^{\frac{1}{8}}}{\left(\frac{4\pi vt}{3B_0Le^{-1}}\right)^{\frac{3}{2}}} \cdot \exp\left[-Le^{-1}vt\right] F\left[vtB_0Le^{-1}\left(1-\frac{r^2}{v^2t^2}\right)^{\frac{3}{4}}\right], \quad \text{(A1)}$$

where

$$F\ [x] = e^x\sqrt{1+2.026/x} \quad \text{(A2)}$$

r is the source receiver distance, W_0 is the source energy, δ is the Dirac's delta, H is the Heaviside function. In this paper function arguments are closed by square brackets while algebraic groupings are inside round brackets. Independent variables are r and t, while the parameters characterizing the area under study are v, B_0 and Le.

Equation 2 is integrated in three intervals:

$$IE_i\ [r] = \int_{r/v+(i-1)\Delta}^{r/v+i\Delta} E\ [r,t]\,\mathrm{d}t \quad \text{(A3)}$$

for I $\in$ {1, 2, 3} and normalized for

$$I\ E_n = \int_{t_c}^{t_c+\Delta_c} E\ [r,t]\,\mathrm{d}t, \quad \text{(A4)}$$

where Δ and Δ_c are time intervals, selected by the analyst, of the order of some seconds; t_c is a time value, measured from the origin time, selected once from the analyst for the whole data set. We selected $t_c = 45$ s , $\Delta = \Delta_c = 12$ s. The normalized three integrals, $\frac{IE_1[r]}{IE_{n[r]}}$, $\frac{IE_2[r]}{IE_n[r]}$ and $\frac{IE_3[r]}{IE_n[r]}$ are finally corrected for geometrical spreading, multiplying for $4\pi r^2$.

Correspondent experimental data are the three integrals of the seismogram Energy Envelopes. Differently from the routine procedure based on calculating the root mean square of the filtered seismograms and summing these values in three time windows (Sato *et al.* 2012), we estimate the quantities in eqs (4) and (5), in a given frequency band centred in f_c calculating the smoothed (using a 10 points moving average, shifting each step by 5 points) Fourier Transform of the velocity seismogram, averaged over the two horizontal components of the ground motion, in three time windows corresponding to the three time windows defined by the integration intervals. It can be demonstrated that the two procedures are equivalent, the present being faster. In this way we calculate four observed values for each source receiver couple and $OE_1[r_k]$, $OE_2[r_k]$, $OE_3[r_k]$ and $OE_c[r_k]$, where r_k is the kth source receiver distance and k spans all the source–receiver couples available.

Ratios $\frac{OE_1[r_k]}{OE_c[r_k]}$, $\frac{OE_2[r_k]}{OE_c[r_k]}$, $\frac{OE_3[r_k]}{OE_c[r_k]}$ corrected for geometrical spreading $4\pi r_k^2$ constitute the observed data.

The fit between theoretical and experimental quantities yields the parameters which characterize the zone (B_0 and Le). We use the L^2 norm, minimizing the squared sum of residuals between observed and theoretical values.

APPENDIX B

The numerical synthesis of the Seismogram Energy Envelopes done following the numerical scheme of Yoshimoto (2000) in the multiple scattering assumption can be calculated in assumptions on the velocity- and heterogeneity–depth distribution more extended than those at the base of the analytical solution by Paasschens (1997). To check how much the half-space assumption affect the estimates done using MLTWA we thus suppose the earth model constituted by a inhomogeneous crust overlying a transparent mantle. In this assumption velocity is assumed depth-dependent through a continuous function of the depth, $v = v(h)$; Moho discontinuity is approximated by a sharp velocity increase around the crust–mantle boundary; inhomogeneity in the crust is parametrized through a depth-dependent scattering coefficient: $\eta_s = \eta_0 f[h]$, where h represents the depth, and η_0 is the scattering coefficient at surface; intrinsic attenuation coefficient is instead assumed independent of depth. Generating a set of synthetic energy envelopes as a function of lapse time and distance in the inhomogeneous model, for reasonable values of B_0 and Le, we span a wide range of values including most of the measurements done through the world. Then, we apply the ordinary MLTWA technique (in the half-space assumption) to these synthetic envelopes. The mathematical relationship between the estimates of B_0 and Le, obtained assuming half-space, with the correspondent values used in the simulation is finally searched, resulting in a second-order polynomial. The coefficients of this polynomial give the correspondence map between the attenuation parameters associated with the uniform model and the attenuation parameters characteristic of a more realistic structure. This map is useful to reinterpret all the couples B_0 and Le calculated in the half-space assumption when the geological structures in which data are recorded are similar to the one adopted in the simulation.